Electronic Supplementary Information for:

Reaction of nitrocefin with two serines of *Pseudomonas aeruginosa* penicillin-binding-protein 3

Hector Newman,[a] Dom Bellini,[b] Alen Krajnc,[c, d] Anthony Tumber,[c] Julie A. Tod,[a] Adrian J. Lloyd,[a] Christopher J. Schofield,*[c] Christopher G. Dowson*[a]

[a]*School of Life Sciences, University of Warwick, Gibbet Hill Road, Coventry, CV4 7AL, United Kingdom.*
[b]*MRC Laboratory of Molecular Biology, Francis Crick Avenue, Cambridge Biomedical Campus, CB2 0QH, United Kingdom.*
[c]*Department of Chemistry and the Ineos Oxford Institute of Antimicrobial Research, Chemistry Research Laboratory, 12 Mansfield Road, Oxford, OX1 3TA, United Kingdom.*
[d]*Faculty of Pharmacy, University of Ljubljana, Askerceva cesta 7, 1000 Ljubljana, Slovenia.*

** Corresponding Authors: C.G.Dowson@warwick.ac.uk christopher.schofield@chem.ox.ac.uk*

Contents:

Experimental Section

Recombination Protein Production and Purification

Cloned, expressed and purified truncated PBP constructs lacking the *N*-terminal transmembrane helix of the *ftsI* genes encoding for penicillin-binding-proteins 3 (PBP3s) were from *Pseudomonas aeruginosa* (PaPBP3, residues 50-579), *Acinetobacter baumannii* (AbPBP3, residues 64-609), and *Escherichia coli* (EcPBP3, residues 60-588). DNA sequences for cloning of PaPBP3 and EcPBP3 were amplified by PCR from genomic DNA; AbPBP3 constructs were synthesized by Integrated DNA Technologies. All mutations in PaPBP3 were introduced using the Qiaquick protocol. All constructs were subcloned into the pET47b vector using restriction enzymes BamHI and HindIII, except for PaPBP3 for which BamHI and SacI restriction enzymes were utilized. Recombinant proteins were expressed and purified using the protocols described below.

Chemically competent *E. coli* BL21-DE3 cells (50 µL) were transformed with the desired expression construct by incubation with the plasmid (1 µL of ~ 150 ng/µL) on ice for 30 minutes followed by heat shock (42 °C for 45 seconds) and further incubation on ice (5 minutes). 400 µL of SOC media (2% (w/v) tryptone, 0.5% (w/v) yeast extract, 10 mM NaCl, 2.5 mM KCl, 10 mM $MgCl_2$, 10 mM $MgSO_4$, 20 mM glucose) was added and the bacteria were allowed to grow (37 °C, 1 hour, 180 rpm shaking). This inoculum (100 µL) was then spread onto agar plates containing kanamycin (50 µg/mL) and grown overnight (37 °C). A single colony from the plate was picked and used to inoculate lysogeny broth (LB) containing kanamycin at 50 µg/ml, which was then allowed to grow as a starter culture overnight (37 °C, 180 rpm shaking). The following day, 3 x 1 L of LB (containing kanamycin at 50 µg/mL) were inoculated each with 10 mL of the overnight culture and allowed to grow to an optical density ($A_{600\ nm}$) of 0.6 in baffled flasks (37 °C, 180 rpm shaking). The cultures were then cooled to 20 °C and PBP3 expression was induced with 1 mM of isopropyl β-D-1-thiogalactopyranoside (IPTG) and continued overnight (20 °C, 180 rpm shaking).

The next day, cells were pelleted at 9,000 x g in a Beckman JLA 8.1000 rotor for 20 minutes at 4 °C. The cell pellet was resuspended in lysis buffer (20 mM sodium phosphate pH 8, 500 mM NaCl, 20 mM imidazole (binding buffer), supplemented with 5 mg/mL lysozyme and 0.5 mg/ml bovine DNase) and then lysed by ultrasonication (10 x 30 s bursts interspersed by a 30 s cooling on ice), using a Bandelin Electronic sonicator. Centrifugation (30,000 x g for 30 minutes at 4 °C in a Beckman JA 25.50 rotor) was used to remove cell debris. All subsequent chromatographic steps were performed at room temperature, at a flow rate of 3 mL/min: the supernatant was loaded onto a 5 ml HisTrap FF Crude column (Cytiva) previously equilibrated with binding buffer + 10 % (w/v) glycerol; the protein was then eluted with a gradient of 10 % to 100 % of elution buffer (20 mM sodium phosphate pH 8, 500 mM NaCl, 500 mM imidazole, 10 % (w/v) glycerol). Proteins prepared for crystallography were additionally purified by reversed nickel affinity chromatography using recombinant HRV 3C protease for tag cleavage. Dialysis was used to exchange the protein solution into a storage buffer (20 mM sodium phosphate pH 8, 500 mM NaCl, 20 % (w/v) glycerol) before making small aliquots and flash-freezing. Protein concentrations were determined by absorbance at 280 nm on a NanoDrop (Thermo Scientific) using a calculated extinction coefficient from ProtParam.[1] Purity (> 95%) was confirmed by gel electrophoresis (Fig. S1).

Proteins were additionally checked for activity by reaction with BOCILLIN FL. 7.5 µg of each protein was reacted with 1 µM of BOCILLIN FL for 20 minutes in 50 mM *bis*-tris propane (Merck) pH 8.5, 75 mM NaCl, 1 % (v/v) DMSO, before the reaction was terminated by the addition of SDS loading dye. The gels were rinsed in water then imaged by a Typhoon FLA 9500 (Cytiva) imager with a 473 nm excitation laser and a 510 nm emission filter (LPB - 510LP) (Fig. S1).

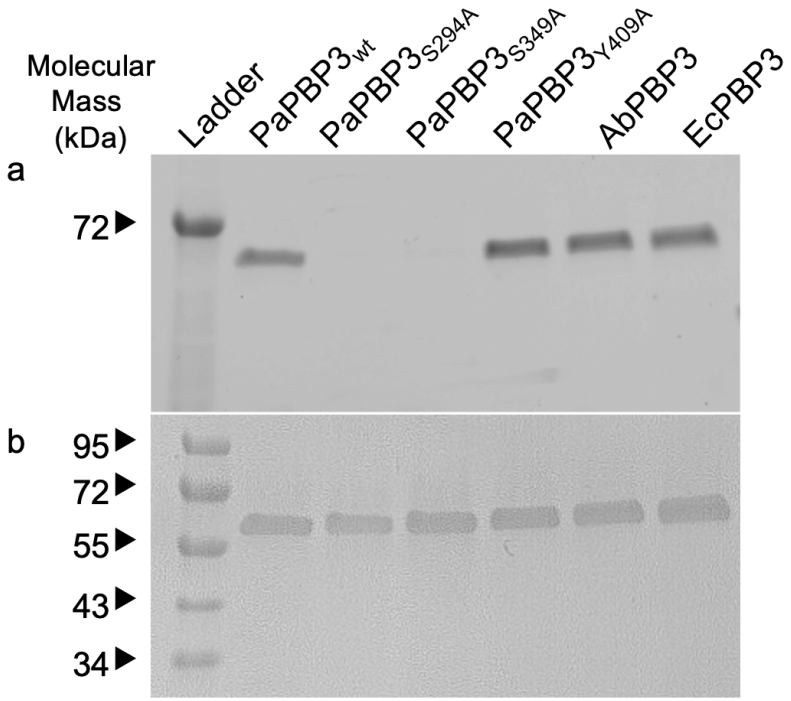

Fig. S1 BOCILLIN FL (a) and Coomassie (b) staining of an SDS-PAGE gel of proteins investigated in this study. (a) BOCILLIN FL (1 µM) was reacted with each PBP (7.5 µg) for 20 minutes before the reaction was terminated by the addition of SDS. Fluorescence was measured using a Typhoon FLA 9000. The standards ladder (Color Prestained Protein Standard ladder, New England Biolabs) has a fluorescent marker protein at 72 kDa. (b) Coomassie staining was carried out on the same gel after the fluorescence was measured. Th gel is representative of 2 replicates.

Crystallisation and Structure Solution

Diffraction quality crystals of $PaPBP3_{wt}$ and$PaPBP_{Y409A}$ were obtained at 294 K using the hanging drop vapour diffusion method from mixing equal volumes of protein with a precipitant solution made up of 25 % (w/v) polyethylene glycol 3350, 0.1 M bis-tris propane, 1 % (w/v) protamine sulphate, pH 8.[2] Crystals were cryoprotected with glycerol (20 % (v/v)) prior to flash-cooling in liquid nitrogen. Nitrocefin-protein complexes were obtained by soaking crystals with 10 mM compound for 60 minutes. Diffraction data were collected at Diamond beamlines I03 and I04. Structures were phased using molecular replacement with MrBump.[3] All data sets were processed using Dials.[4] Manual interactive building and ligand fitting was performed with Coot.[5] Structures were refined with REFMAC5 and validated with MolProb.[6,7] Figures of structures were prepared with PyMOL (The PyMOL Molecular Graphics System, Schrödinger, LLC) or CCP4mg.[8]

Denaturing Mass Spectrometry

Denaturing mass spectrometry analyses of PBP3-WT and the Y409A mutant were performed by Liquid Chromatography Mass Spectrometry (LCMS) using an Agilent 1290 infinity II LC system equipped with an Agilent 1290 multisampler (G7167B) and an Agilent 1290 high speed pump (G7120A). The LC system was connected to an Agilent 6550 accurate mass iFunnel quadrupole time of flight (QTOF) mass spectrometer. 1 µM of protein was reacted with 10-100 µM of nitrocefin in 50 mM ammonium acetate buffer, pH 7.0. Reaction samples (10 µL) were injected after the specified time points and loaded onto a ProSwift™ RP-4H analytical column (Thermo Scientific). Solvent A consisted of LCMS grade water containing 0.1% (v/v) formic acid and solvent B consisted of acetonitrile containing 0.1% (v/v) formic acid. Protein was separated using a step wise gradient (0 min - 95% solvent A, 1.0 min - 80% solvent A, 1.5 min - 45% solvent A, 3.0 min - 0% solvent A, 4.0 min - 0% solvent A, 5.0 min - 95% solvent A). This was followed by a 3 min post run with 95% solvent A to re-equilibrate the column, all flow rates were 0.2 mL/min. The mass spectrometer was operated in the positive ion mode with a drying gas temperature (225 °C), drying gas flow rate (13 L/min), nebulizer pressure (40 psig), sheath gas temperature (350 °C), sheath gas flow rate (12 L/min), capillary voltage (4000 V), nozzle voltage (1000 V).

The S294A and S349A variants were analysed by solid phase extraction mass spectrometry (SPE-MS) using an Agilent RapidFire RF365 high throughput sampling robot connected to an Agilent 6550 accurate mass iFunnel quadrupole time of flight (QTOF) mass spectrometer. Protein (1 µM) was reacted with 10 µM of nitrocefin in 50 mM ammonium acetate buffer, pH 7.0. Samples analysed every minute by injection under vacuum onto a C4 SPE cartridge at a flow rate of 1.5 mL/min. The C4 SPE cartridge was then washed for 5.5 sec with LCMS water containing 0.1% (v/v) formic acid at a flow rate of 1.5 mL/min to remove non-volatile buffer salts. Proteins were then eluted from the C4 SPE cartridge in an organic solvent (85% (v/v) acetonitrile, 15% (v/v) LCMS water containing 0.1% (v/v) formic acid) at a flow rate of 1.25 mL/min for 5.5 sec. The mass spectrometer was operated in the positive ion mode with a drying gas temperature (225 °C), drying gas flow rate (13 L/min), nebulizer pressure (40 psig), sheath gas temperature (350 °C), sheath gas flow rate (12 L/min), capillary voltage (4000 V), nozzle voltage (1000 V).

All acquired data were analysed using Agilent MassHunter Qualitative Analysis (Version B.07.00) software. Protein spectra acquired in profile data format were deconvoluted using the maximum entropy deconvolution algorithm.

Kinetic Assays

Measurements were carried out at 30 °C in triplicate using a Hellma micro quartz cuvette (1 cm pathlength) in a Cary 100 UV/vis spectrophotometer (Agilent) using a 1 nm slit band width. Data were acquired every 0.1 s. Nitrocefin (Abcam) or CENTA ((6*R*,7*R*)-3-(((3-carboxy-4-nitrophenyl)thio)methyl)-8-oxo-7-(2-(thiophen-2-yl)acetamido)-5-thia-1-azabicyclo[4.2.0]oct-2-ene-2-carboxylic acid, Calbiochem) in a buffer of 50 mM *bis*-tris propane pH 8.5, 75 mM NaCl, 1 % (v/v) DMSO (Merck) was added to the cuvette before the protein (in the same buffer) was added to initiate reaction. The final volume in the cuvette was 200 µL. The initial rate immediately after mixing was measured using the spectrophotometer software. A dead time of ~ 10 s occurred whilst the substrates were mixed and the measurement initiated. Background turnover due to non-enzymatic hydrolysis of nitrocefin or CENTA were measured in parallel and subtracted from the rates. Reactions with nitrocefin were followed at 482 nm ($\varepsilon_{1\text{ cm, }482\text{ nm}}$ = 17,400 $M^{-1}\cdot cm^{-1}$)[9] and reactions with CENTA were followed at 405 nm ($\varepsilon_{1\text{ cm, }405\text{ nm}}$ = 6,400 $M^{-1}\cdot cm^{-1}$)[10]. The specific rates (reaction velocity divided by the concentration of enzyme (equation 6.S3)) were fitted to either S1 or Equation S2 using non-linear regression in Prism 9 (GraphPad Software), and the best fit parameters are reported with the standard errors of the mean.

Protein concentrations were chosen such that the turnover rate was at least 10-fold higher than the background nitrocefin turnover rate. For reactions with nitrocefin, the protein concentrations were: $PaPBP3_{wt}$: 0.4 µM; $PaPBP3_{S349A}$: 2.4 µM; $PaPBP3_{Y409A}$: 2.4 µM; AbPBP3: 0.8 µM; EcPBP3: 1.8 µM. Turnover rates were linear with respect to the protein concentration (Fig. S9b). For the reaction with CENTA, 0.8 µM of $PaPBP3_{wt}$ was used. For $PaPBP3_{S294A}$, conditions for steady state turnover at a sufficient rate were not identified (up to 10 µM was tested).

The upper limits for concentrations of substrates were determined by the solubility of the substrate. Partial solubility was observed > 500 µM of nitrocefin and > 1 mM of CENTA. ~ 2-fold less than this was used to ensure insolubility was not causing the observed effects. The lowest concentration of nitrocefin tested was always > 10-fold higher than the protein concentration.

Kinetic Analysis

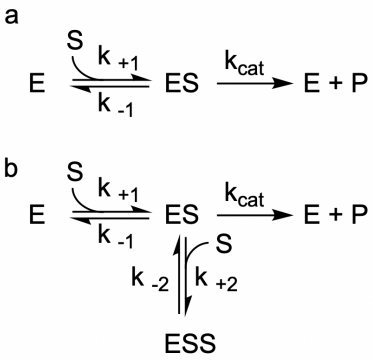

Scheme S1 Schemes for reaction without (a) and with substrate inhibition (b). E: enzyme; S: substrate; ES: enzyme: substrate complex with one substrate bound; P: product; ESS: enzyme: substrate complex with two molecules of substrate bound. (b) shows a substrate inhibition scheme in which the second substrate can only bind to the ES complex and the ESS complex does not yield a product directly.

Graphs plotting the enzyme velocity for each of the enzyme-substrate reactions were fit to one of the kinetic models, without (Scheme S1a)[11–13] or with substrate inhibition (Scheme S1b)[12,14,15]. In substrate inhibition kinetics, a non-hyperbolic relationship is observed with increasing substrate concentration, where there is a maximum rate attained at a given substrate concentration, above which, it declines.

For simple saturation kinetics, plots of velocity (*v*) against concentration of substrate (*[S]*) were fit (using GraphPad 9 for MacOS) using equation S1 to obtain values for V_{max} and K_M.

$$v = \frac{V_{max}\,[S]}{K_M\, + [S]} \qquad \textbf{(S1)}$$

For substrate inhibition kinetics, plots of velocity (*v*) against concentration of substrate (*[S]*) were fit (using GraphPad 9 for MacOS) using equation S2 to obtain values for V_{max}, K_M and K_{SI}.

$$v = \frac{V_{max}\,[S]}{K_M\, + [S](1\, + \frac{[S]}{K_{SI}})} \qquad \textbf{(S2)}$$

Where V_{max}, K_M and K_{SI} are related to the rate constants in Scheme S1 by the following equations:

$$K_M = \frac{k_{-1} + k_{cat}}{k_{+1}} \quad \textbf{(S3)}$$

$$K_{SI} = \frac{k_{-2}}{k_{+2}} \quad \textbf{(S4)}$$

$$V_{max} = k_{cat} \cdot [E] \quad \textbf{(S5)}$$

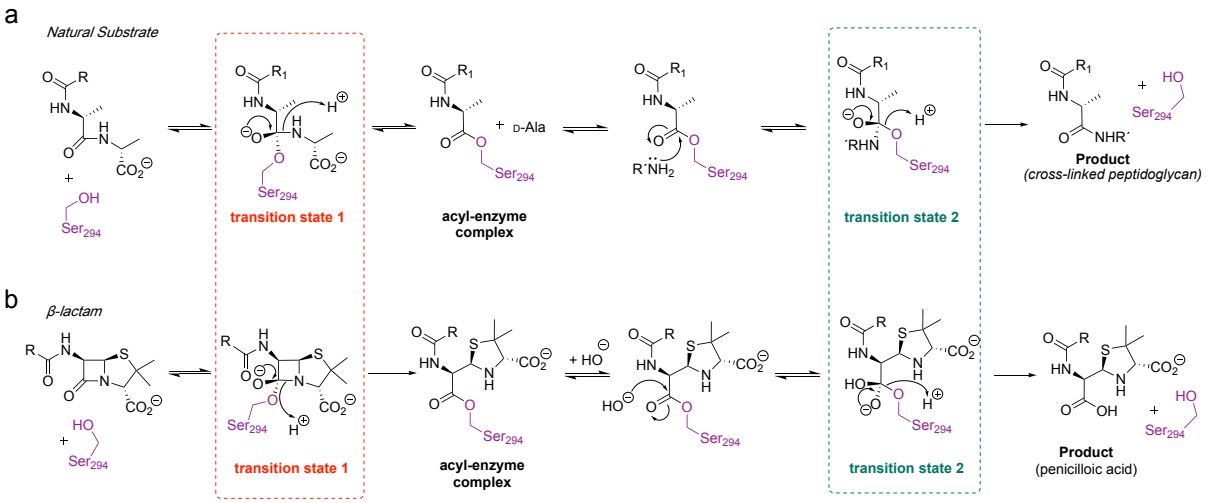

Scheme S2 Outline of general mechanisms of the natural product reactions carried out by the transpeptidase domains of PBPs (including *P. aeruginosa* PBP (PaPBP3)) and the reaction of a β-lactam (exemplified with penicillin) with a PBP. Residue numbering refers to PaPBP3. (a) The peptidoglycan stem peptide (the "donor"), with its terminal D-Ala-D-Ala motif enters the active site, forming a non-covalent complex, which is attacked by the nucleophilic serine (here Ser294) to form an acyl-enzyme complex, concomitant with release of the terminal D-Ala. Subsequent attack by a second nucleophile (the "acceptor") leads to formation of the crosslinked peptidoglycan product. In transpeptidation reactions of Gram-negative organisms, the acceptor nucleophile is the ε-amine of a meso-diaminopimelyl (DAP) residue (the 3rd amino acid in an adjacent stem peptide). Hydrolysis of the acyl-enzyme complex can also occur.[16] (b) Serine β-lactamases use an analogous mechanism to hydrolyse β-lactams. For PBPs, the hydrolysis of the β-lactam acyl-enzyme complex is typically slow (< 0.02 min^{-1}) [17–20], but rapid in β-lactamase-mediated hydrolysis. Structural analogy between the β-lactams and the stem peptide D-Ala-D-Ala (Tipper-Strominger hypothesis) is thought to contribute to PBP inhibition by β-lactams.[21]

Table S1. Crystallographic data collection and refinement statistics.

Dataset	$PaPBP3_{wt}$ reacted with nitrocefin PDB Code: 6HR6	$PaPBP3_{Y409A}$ reacted with nitrocefin PDB Code: 6HR9
Beamline	DLS I04	DLS I04
Wavelength	0.9795	0.9795
Resolution range[a]	2.53-52.98 (2.53-2.57)	1.99-60.72 (1.99-2.02)
Space group	P 21 21 21	P 21 21 21
Unit cell	68.68 83.27 89.10 90 90 90	68.04 83.26 88.73 90 90 90
Unique reflections[a]	17652 (858)	35268 (1688)
Multiplicity[a]	8.5 (7.9)	8.4 (8.1)
Completeness (%)[a]	100 (98.3)	100 (97.9)
Mean I/sigI[a]	7.8 (1.9)	9.1 (1.9)
Rmeas	0.19 (0.97)	0.13 (0.90)
CC½[a]	1.0 (0.4)	1.0 (0.6)
R_{work}	0.23	0.22
R_{free}	0.29	0.28
RMS bonds (Å)	0.008	0.009
RMS angles (°)	1.660	1.542
Average B-factor (Å^2)	56.54	42.68
Number of non-hydrogen atoms		
overall	3894	3904
ligands	35	70
solvent	8	83
Molprobity score	2.26	1.96
Ramachandran outliers	1	0
Rotamer outliers	0	0
Clashscore	21.32	20.12

[a]Parentheses indicate high resolution shell

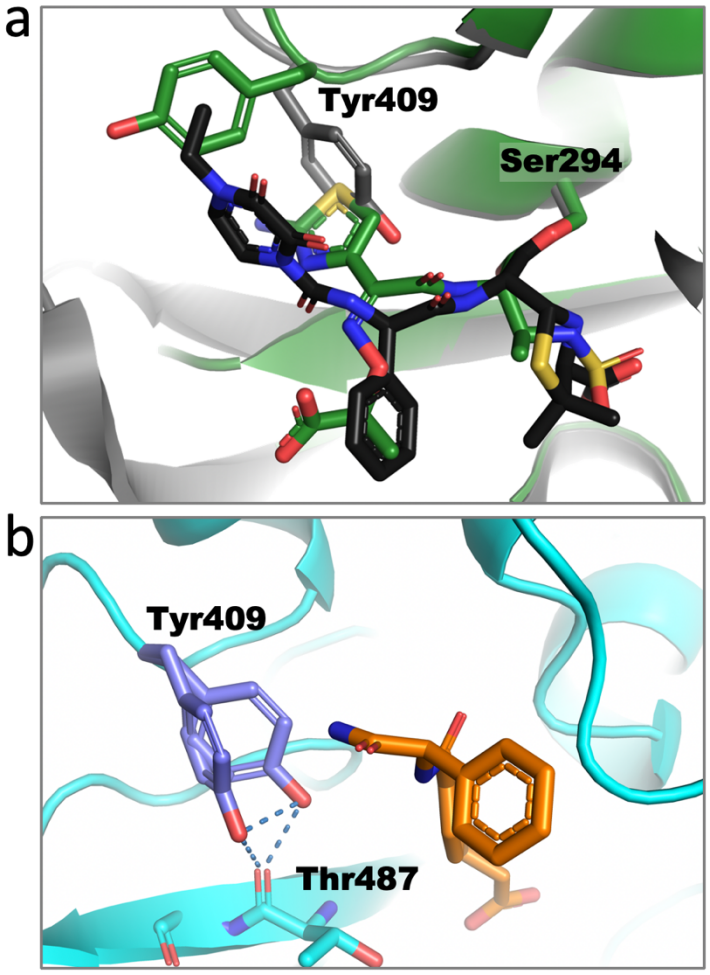

Fig. S2 Tyr409 conformational flexibility in PaPBP3. (a) Comparison of the PaPBP3:aztreonam (green, PDB: 3PBS)[22] and PaPBP3:piperacillin (black, PDB: 6R3X)[23] complex structures. Tyr409 is pointed towards the active site serine in the piperacillin-reacted structure, but faces out of the active site in the aztreonam-reacted structure. (b) View from a structure of PaPBP3 in complex with a benzoxaborole manifests two conformations for Tyr409 (PDB: 7AU1).[24] Both conformations form a hydrogen bond with the Thr487 backbone carbonyl group.

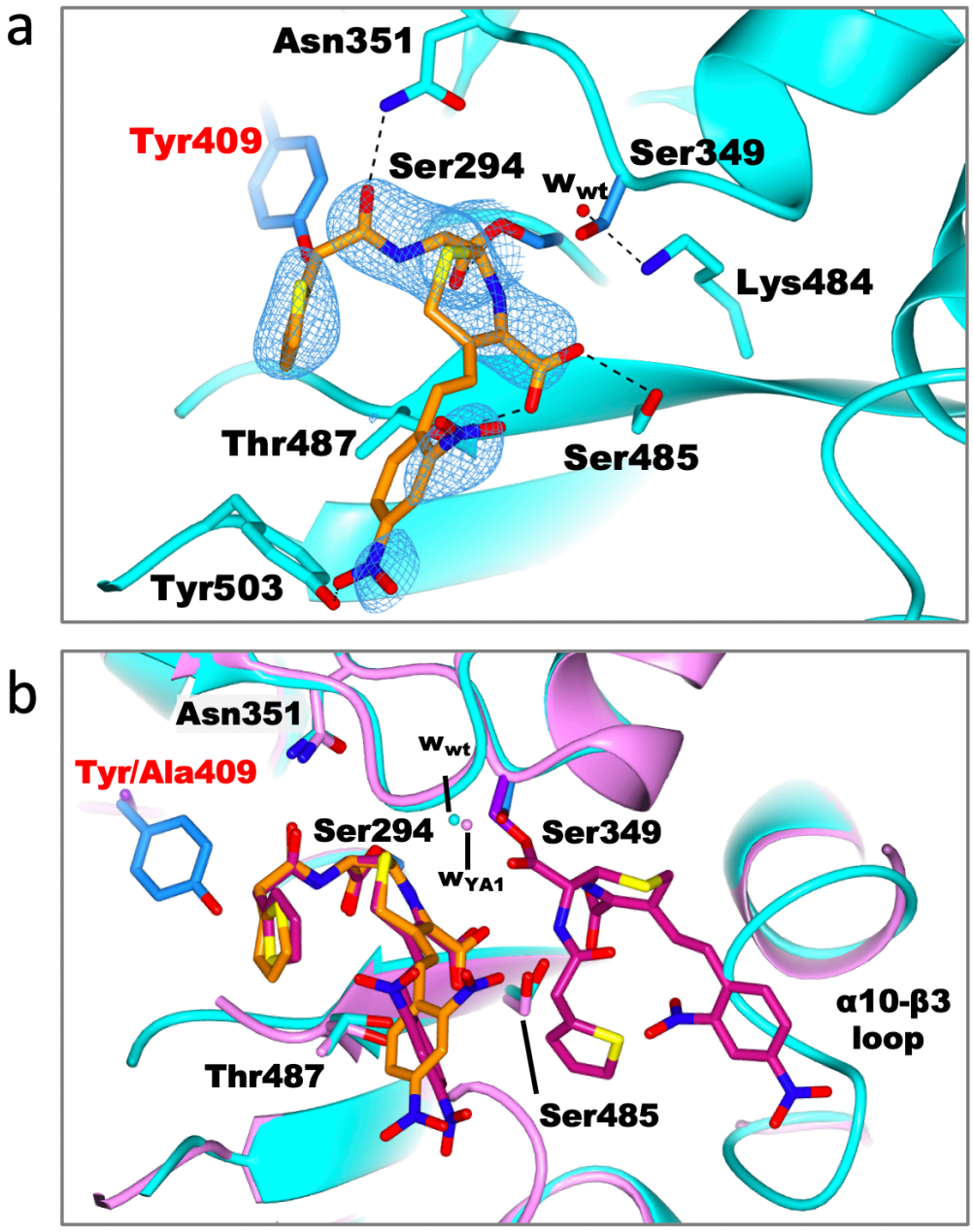

Fig. S3 Electron density of nitrocefin-reacted PaPBP3$_{wt}$ (a PBP3$_{wt}$ protein is in cyan and the reacted nitrocefin-derived ligand in orange) (a) and comparison of the active sites of crystal structures of PaPBP3$_{wt}$ and PaPBP$_{Y409A}$ reacted with nitrocefin (b) (PaPBP3$_{Y409A}$ protein is in pink and the reacted nitrocefin-derived ligands in purple). Nitrocefin reacts with Ser294 in the PaPBP3$_{wt}$ structure, and with Ser294 and Ser349 (separately) in the PaPBP$_{Y409A}$ structure. Neighbouring residues are labelled sticks. Hydrogen bonds (black dashed lines in panel (a)) are shown from the nitrocefin-derived ligands to nearby residues. In the PaPBP3$_{wt}$ structure, only one of the two refined conformations of Ser349 is shown. A water molecule (w_{wt} and w_{YA1} for the structures with PaPBP3$_{wt}$ and PaPBP$_{Y409A}$ respectively) is positioned similarly in the active sites of both structures.

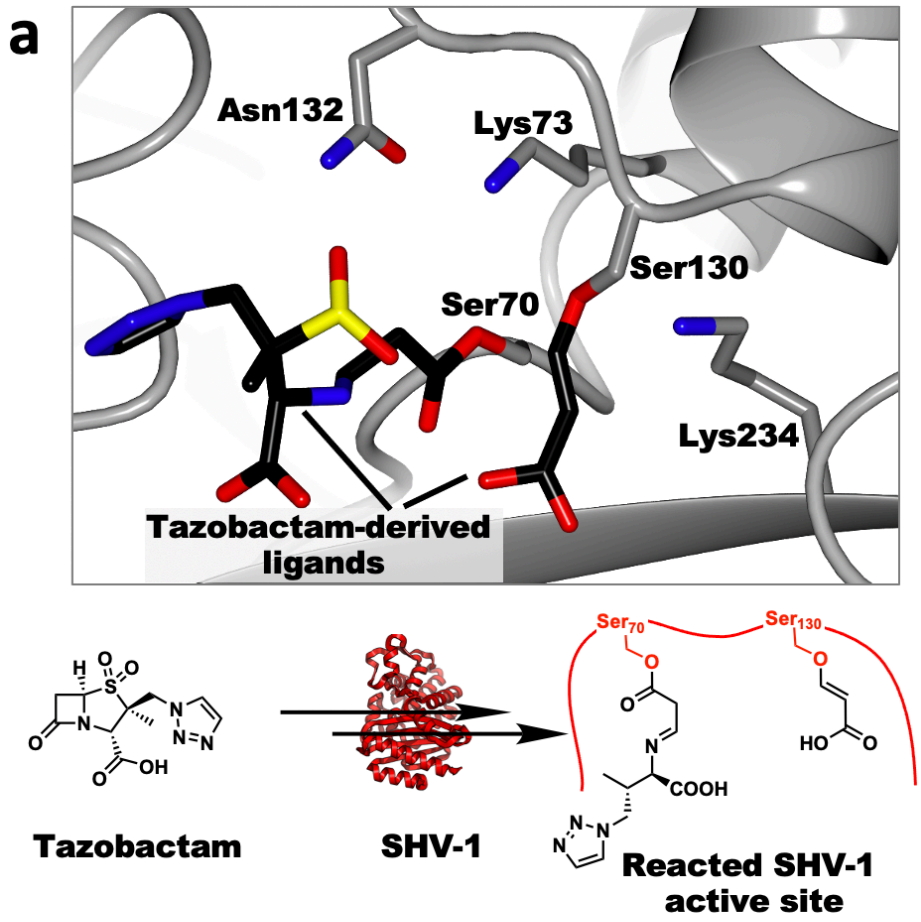

Fig. S4 Reaction of tazobactam with SHV-1 (PDB: 1VM1).[25] (a) Two different fragments derived from tazobactam (black) were reported to separately bind to both Ser70 and Ser130 of SHV-1 (grey). (b) Comparison of the binding modes of nitrocefin-derived molecules from $PaPBP3_{Y409A}$ (PDB: 6HR9, orange and cyan) and the tazobactam-derived ligands binding SHV-1 (black and grey).

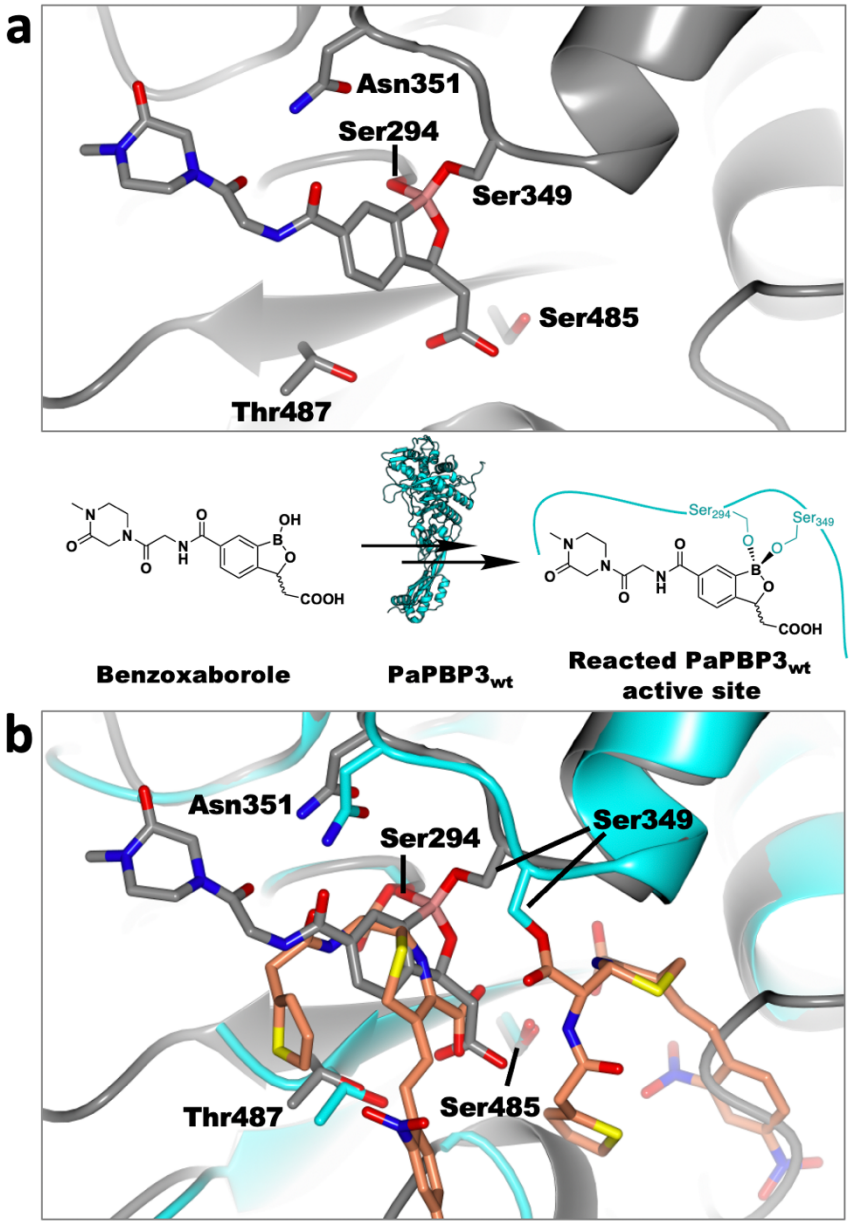

Fig. S5 Benzoxaboroles bind to PaPBP3, reacting with both Ser294 and Ser349 (PDB: 7AU8).[24] (a) Binding mode of a benzoxaborole with PaPBP3$_{wt}$ (grey), neighbouring residues are sticks and are labelled. The boron atom of the benzoxaborole is bound to both Ser294 and Ser349. (b) Comparison of the binding modes of nitrocefin-derived molecules from PaPBP3$_{Y409A}$ (PDB: 6HR9, orange and cyan) and the PaPBP3:benzoxaborole complex (grey). Note that the side chain of Ser349 is rotated ~108° between the two structures.

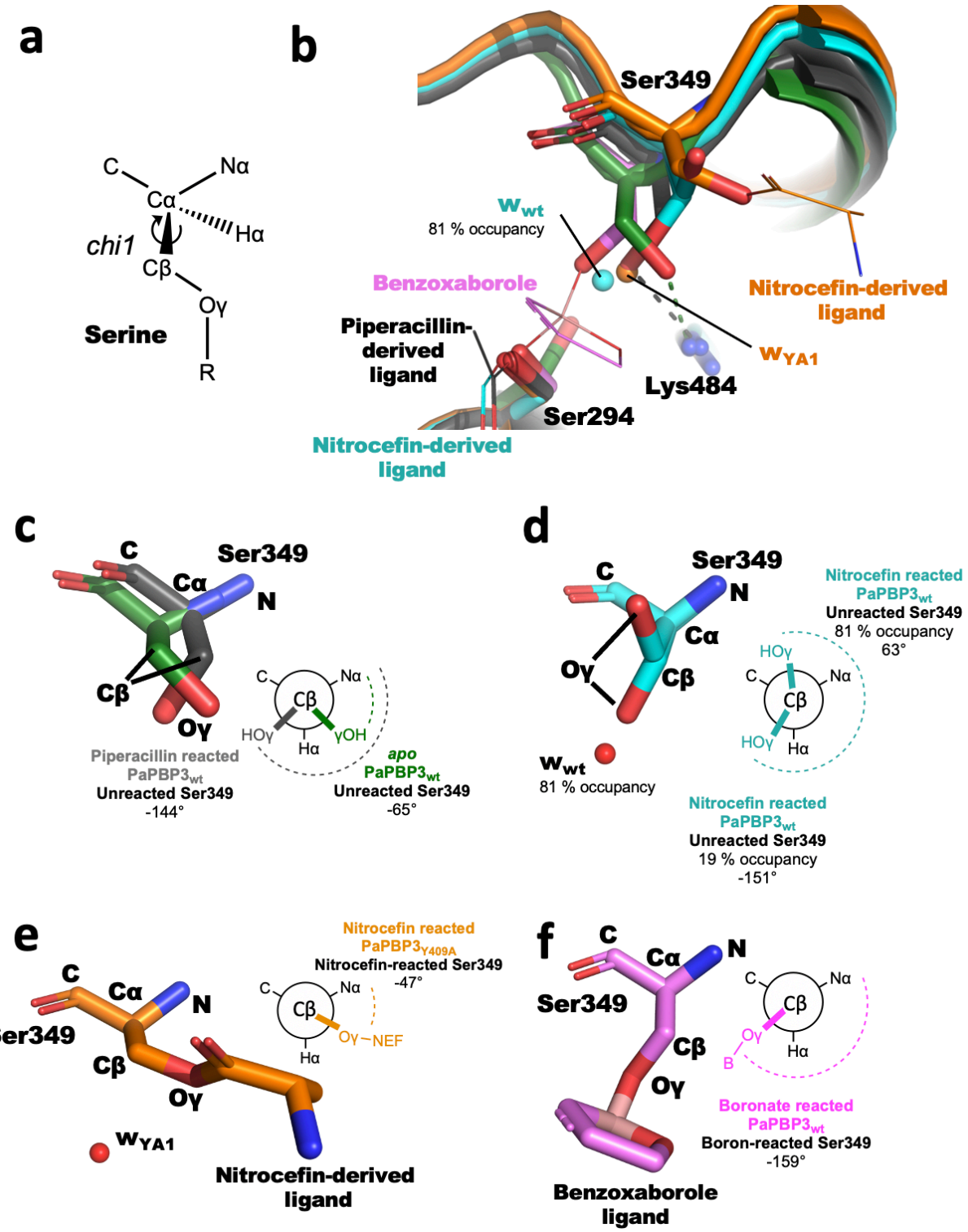

Fig. S6 Conformations of Ser349 in PaPBP3 crystal structures. (a) Labels of serine atoms. (b) Overlays of Ser349 conformations from: *apo* $PaPBP3_{wt}$ (green, PDB: 6HZR[23]); piperacillin-reacted $PaPBP3_{wt}$ (grey, PDB: 6R3X[23]); nitrocefin-reacted $PaPBP3_{wt}$ (cyan, PDB: 6HR6); nitrocefin-reacted $PaPBP3_{Y409A}$ (orange, PDB: 6HR9); benzoxaborole-reacted $PaPBP3_{wt}$ (pink, PDB: 7AU8[24]). Ligands are shown as lines and are truncated for clarity. Hydrogen bonds are shown between Ser349 and Lys484 in: piperacillin-reacted $PaPBP3_{wt}$ (black) and *apo* $PaPBP3_{wt}$ (green). Waters W_{wt} and W_{YA1} from nitrocefin-reacted $PaPBP3_{wt}$ (cyan, PDB: 6HR6) and nitrocefin-reacted $PaPBP3_{Y409A}$ (orange, PDB: 6HR9) respectively are shown near to Ser349. Sidechains for Ser294 and Lys484 are shown. (c-f) Conformations and Newman projections of Ser349 for each of the structures shown in (b). Angles are measured from the backbone amine nitrogen (**N**), Newman projections are along the Cα-Cβ bond. (b and d) In nitrocefin-reacted $PaPBP3_{wt}$ (PDB: 6HR6) two conformations of Ser349 were modelled into the density, differentiated by the *chi1* angle of the residue and different occupancies: 81 % at 63° and 19 % at -151° (relative to the backbone amine). A water (W_{wt}) is modelled at 81 %, presumed to be present in the active site at the same time as the corresponding alternate conformer. (e) NEF indicates the position of the reacted nitrocefin ligand which is truncated in the image for clarity. (f) B indicates the position of the benzoxaborole, the view of which is truncated for clarity (Fig. S5).

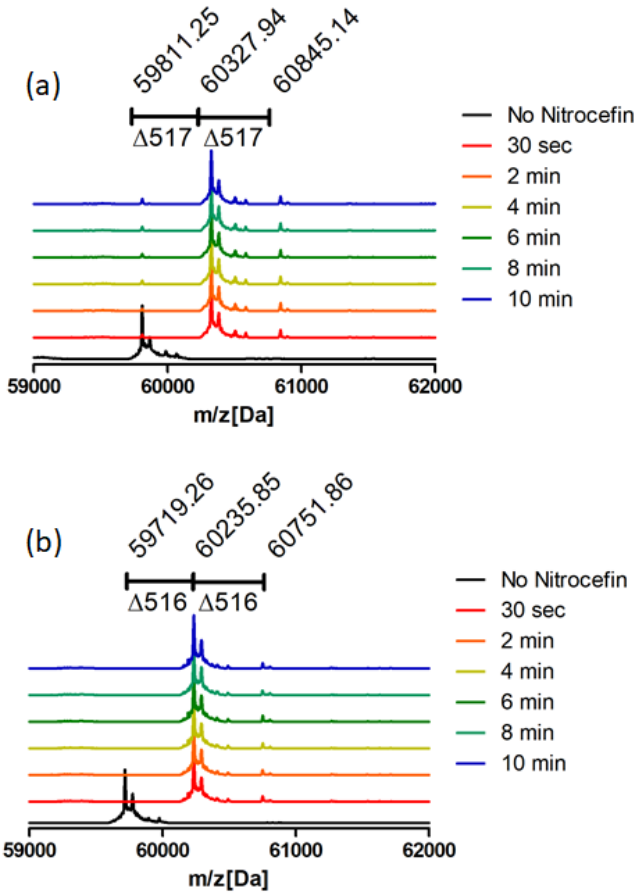

Fig. S7 Liquid Chromatography Mass Spectrometric (LCMS) analysis of the reactions of $PaPBP3_{wt}$ (a) and $PaPBP3_{Y409A}$ (b) (both 1 µM) with nitrocefin (10 µM). Deconvoluted mass spectra show masses corresponding to the protein ion for (a) $PaPBP3_{wt}$, predicted unreacted mass (from sequence): 59809.29 Da, observed 59811.25 Da and (b) $PaPBP3_{Y409A}$, predicted unreacted mass: 59717.19 Da, observed 59719.26 Da. Additional peaks correspond to adducts of nitrocefin (calculated incremental Δmass: 516.50 Da). For both proteins, a PBP-nitrocefin complex was formed within 30 s.

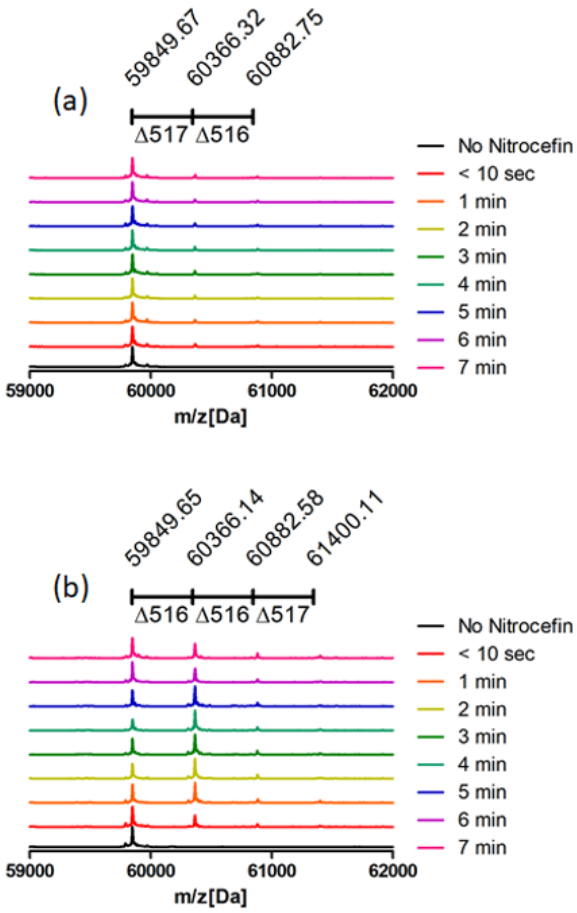

Fig. S8 Solid Phase Extraction Mass Spectrometric (SPE-MS) analysis of the reactions of $PaPBP3_{S294A}$ (a) and $PaPBP3_{S349A}$ (b) (both 1 µM) with nitrocefin (10 µM). Deconvoluted mass spectra show masses corresponding to the protein for (a) $PaPBP3_{S294A}$, observed 59849.67 Da and (b) $PaPBP3_{S349A}$, observed 59849.65 Da. Additional peaks correspond to adducts of one and (to a lesser extent) two nitrocefins are observed with substantially more reaction being observed with $PaPBP3_{S349A}$ (calculated incremental Δmass for one nitrocefin reaction: 516.50 Da). For both proteins, formation of a PBP-nitrocefin complex was formed within 10 s. For both unmodified proteins, a mass of 59793.29 Da was predicted, a deviation from the observed masses by ~56 Da (possibly corresponding to complexation of copurifying Ni with the His-tag.

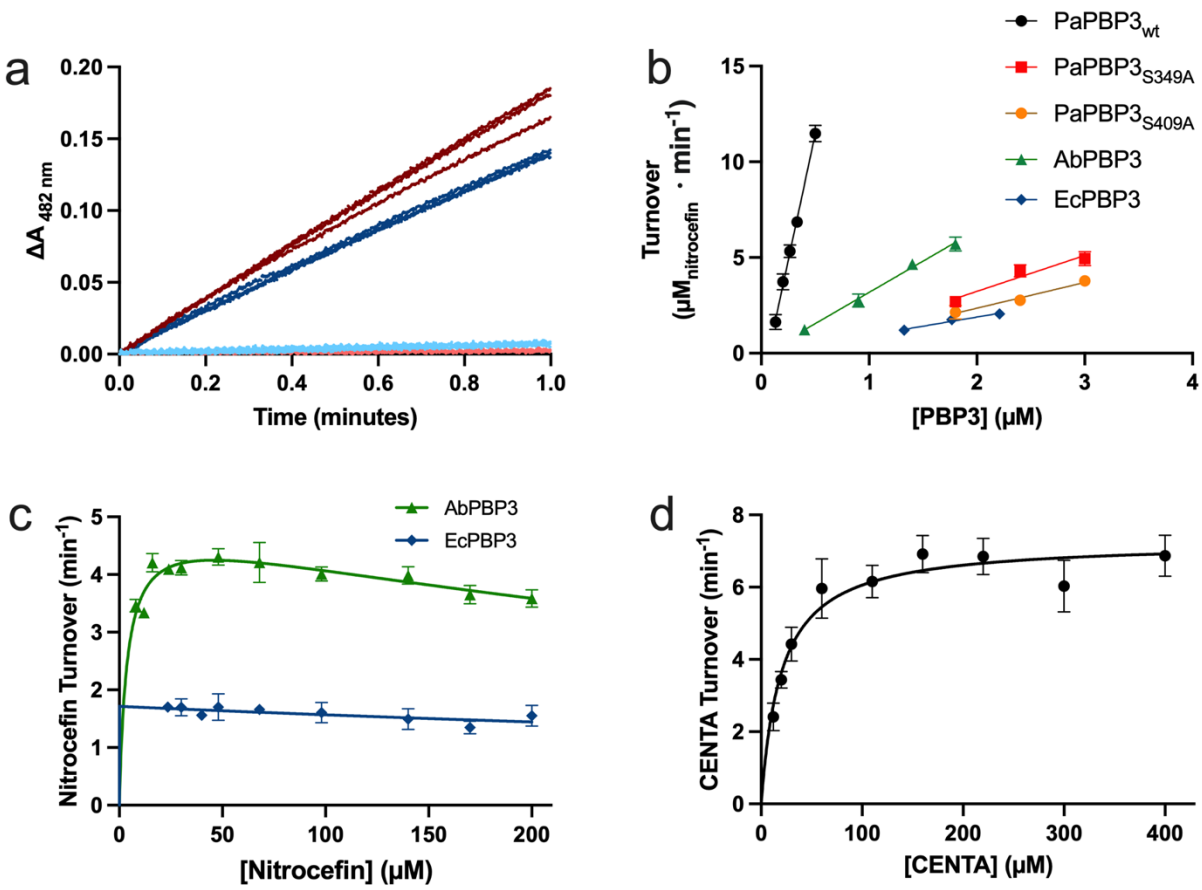

Fig. S9 (a) Change in absorbance at 482 nm due to nitrocefin turnover. Individual readings (n = 3) are plotted as dots. The $PaPBP3_{wt}$-catalysed turnover rate (dark colours) is compared to the background rate (light colours): nitrocefin at 48 μM (red and pink) and nitrocefin at 160 μM (blue and cyan). (b) Relationship between protein concentration and nitrocefin turnover. For each protein studied ($PaPBP3_{wt}$: black circles; $PaPBP3_{S349A}$: red squares; $PaPBP3_{Y409A}$: orange circles; AbPBP3: green triangles; EcPBP3: blue diamonds), there was a linear relationship between the amount of protein in the reaction and the background-corrected turnover rate. Nitrocefin turnover could not be recorded for $PaPBP3_{S294A}$ with up to 10 μM protein. (c) Substrate concentration nitrocefin turnover graphs in the presence of: AbPBP3 (green, triangles, 0.8 μM) and EcPBP3 (blue, diamonds, 1.8 μM). For EcPBP3, the K_M was too low to be determined (< 15 fold above the protein concentration) and the shallow negative gradient of the right hand portion of the graph (-1.4×10^{-3} $min^{-1} \cdot \mu M^{-1}$ compared to -44.6×10^{-3} $min^{-1} \cdot \mu M^{-1}$ for $PaPBP3_{wt}$ (Fig. 3)) also makes it impossible to define the K_{SI} of the interaction accurately. (d) CENTA turnover rates with $PaPBP3_{wt}$ (PBP concentration: 0.8 μM). (b-d) The standard deviation of 3 technical replicates is shown for each point. (c-d) Data points were fitted using a non-linear regression (solid line) in Prism 9 for Mac OS (Graphpad) to equation S2 (c) or equation S1 (d). The best fit parameters are shown in Table 1. For all graphs, the standard deviation of 3 points is shown for each point.

References

1 E. Gasteiger, C. Hoogland, A. Gattiker, S. Duvaud, M. R. Wilkins, R. D. Appel and A. Bairoch, in *The Proteomics Protocols Handbook*, ed. J. M. Walker, Humana Press, Totowa, NJ, 2005, pp. 571–607.

2 S. Sainsbury, L. Bird, V. Rao, S. M. Shepherd, D. I. Stuart, W. N. Hunter, R. J. Owens and J. Ren, *Journal of Molecular Biology*, 2011, **405**, 173–184.

3 R. M. Keegan and M. D. Winn, *Acta Crystallogr D Biol Crystallogr*, 2008, **64**, 119–124.

4 G. Winter, D. G. Waterman, J. M. Parkhurst, A. S. Brewster, R. J. Gildea, M. Gerstel, L. Fuentes-Montero, M. Vollmar, T. Michels-Clark, I. D. Young, N. K. Sauter and G. Evans, *Acta Crystallogr D Struct Biol*, 2018, **74**, 85–97.

5 P. Emsley, B. Lohkamp, W. G. Scott and K. Cowtan, *Acta Crystallogr D Biol Crystallogr*, 2010, **66**, 486–501.

6 A. A. Vagin, R. A. Steiner, A. A. Lebedev, L. Potterton, S. McNicholas, F. Long and G. N. Murshudov, *Acta Crystallogr D Biol Crystallogr*, 2004, **60**, 2184–2195.

7 C. J. Williams, J. J. Headd, N. W. Moriarty, M. G. Prisant, L. L. Videau, L. N. Deis, V. Verma, D. A. Keedy, B. J. Hintze, V. B. Chen, S. Jain, S. M. Lewis, W. B. Arendall, J. Snoeyink, P. D. Adams, S. C. Lovell, J. S. Richardson and D. C. Richardson, *Protein Science*, 2018, **27**, 293–315.

8 S. McNicholas, E. Potterton, K. S. Wilson and M. E. M. Noble, *Acta Crystallogr D Biol Crystallogr*, 2011, **67**, 386–394.

9 M. G. P. Page, *Biochimica et Biophysica Acta (BBA) - Protein Structure and Molecular Enzymology*, 1994, **1205**, 199–206.

10 C. Bebrone, C. Moali, F. Mahy, S. Rival, J. D. Docquier, G. M. Rossolini, J. Fastrez, R. F. Pratt, J.-M. Frère and M. Galleni, *Antimicrob. Agents Chemother.*, 2001, **45**, 1868–1871.

11 G. E. Briggs and J. B. S. Haldane, *Biochemical Journal*, 1925, **19**, 338–339.

12 R. A. Copeland, *Enzymes: a practical introduction to structure, mechanism, and data analysis*, Wiley, New York, 2nd ed., 2000.

13 M. Dixon and E. C. Webb, *Enzymes*, Longman, London, 3. ed., (completely rev.)., 1979.

14 P. M. Kaiser, *Journal of Molecular Catalysis*, 1980, **8**, 431–442.

15 M. C. Reed, A. Lieb and H. F. Nijhout, *Bioessays*, 2010, **32**, 422–429.

16 E. Sauvage, F. Kerff, M. Terrak, J. A. Ayala and P. Charlier, *FEMS Microbiol Rev*, 2008, **32**, 234–258.

17 A. B. Shapiro, R.-F. Gu, N. Gao, S. Livchak and J. Thresher, *Analytical Biochemistry*, 2013, **439**, 37–43.

18 M. Adam, C. Fraipont, N. Rhazi, M. Nguyen-Distèche, B. Lakaye, J. M. Frère, B. Devreese, J. V. Beeumen, Y. van Heijenoort, J. van Heijenoort and J. M. Ghuysen, *Journal of Bacteriology*, 1997, **179**, 6005–6009.

19 J. M. Ghuysen, J. M. Frère, M. Leyh-Bouille, M. Nguyen-Distèche and J. Coyette, *Biochem. J.*, 1986, **235**, 159–165.

20 W.-P. Lu, E. Kincaid, Y. Sun and M. D. Bauer, *Journal of Biological Chemistry*, 2001, **276**, 31494–31501.

21 D. J. Tipper and J. L. Strominger, *Proceedings of the National Academy of Sciences*, 1965, **54**, 1133–1141.

22 S. Han, R. P. Zaniewski, E. S. Marr, B. M. Lacey, A. P. Tomaras, A. Evdokimov, J. R. Miller and V. Shanmugasundaram, *Proceedings of the National Academy of Sciences*, 2010, **107**, 22002–22007.

23 D. Bellini, L. Koekemoer, H. Newman and C. G. Dowson, *J. Mol. Biol.*, 2019, **431**, 3501–3519.

24 H. Newman, A. Krajnc, D. Bellini, C. J. Eyermann, G. A. Boyle, N. G. Paterson, K. McAuley, R. Lesniak, M. Gangar, F. von Delft, J. Brem, K. Chibale, C. J. Schofield and C. G. Dowson, *J. Med. Chem.*, , DOI:https://doi.org/10.1021/acs.jmedchem.1c00717.

25 A. P. Kuzin, M. Nukaga, Y. Nukaga, A. Hujer, R. A. Bonomo and J. R. Knox, *Biochemistry*, 2001, **40**, 1861–1866.